Are Smartphones Suited for DTN Networking?

A methodological teardown of smartphones' WiFi performance

Bernhard Distl
Computer Engineering and Networks Laboratory
ETH Zurich, Switzerland
Email: distl@tik.ee.ethz.ch

Franck Legendre
Uepaa AG
Zurich, Switzerland
Email: franck.legendre@uepaa.ch

***Abstract*—Opportunistic networks are formed by people carrying mobile devices with wireless capabilities. When in mutual transmission range (or contact), nodes of such networks use device-to-device communication to automatically exchange data, without requiring fixed infrastructure. A few apps have already proven opportunistic networking to be a useful communication paradigm. While contacts have been studied theoretically, in practice, they depend to a large extent on the characteristics of the mobile devices, typically smartphones. Up to our knowledge, no study has considered the radio characteristics of current smartphones acting as opportunistic nodes yet. In this paper, we hence investigate the WiFi radio performances of smartphones for opportunistic networking. We start by revisiting the classical link budget by adding the impact of the phone's carrier. We then perform extensive measurements to fully characterize all components of the link budget between two smartphones. We find that the Two-Ray propagation model is the best fit as a smartphone propagation model. Eventually, to assess the capacity of opportunistic networking we evaluate a simple scenario of two pedestrians crossing on a path. In this scenario, we show that a maximum range of more than 400m can be achieved and that during the resulting contact opportunity a total of 171 MB goodput can be transferred.**

I. Introduction

Opportunistic networking or delay-tolerant networking (DTN) appears more and more as a promising additional means of communication [1], [2]. Opportunistic networking happens when two or more devices come into mutual transmission range and exchange data directly with each other. As no infrastructure is required for this exchange, opportunistic networks can be used for cellular offloading [3], communication in disaster situations where the infrastructure is teared down or missing [4] or anti-censorship communications. Yet, the potential of opportunistic networking lies in extending the reach of the Internet to rural and remote areas [5]. Facebook with the Internet.org project and Google with its Project Loon have now rushed into a battle to provide Internet connectivity to the still disconnected 4 billion human beings.

The core element supporting opportunistic networks is smartphones. Already smartphones are reaching to emerging markets and Facebook has partnered with Ericsson to build the first very low cost smartphones for an expected 20-25$ per unit. While the potential for opportunistic networking has already been demonstrated through the N4C project [6] or apps such as Twimight [7], Uepaa [8] and Firechat [9], there is only little scientific evidence of the large-scale potential of opportunistic networking based on smartphones. In practice, the contact opportunities – the building block of opportunistic networks – depend to a large extent on the characteristics of the mobile devices, typically smartphones, that are carried around. Up to now, no study has ever considered the radio characteristics of current smartphones acting as opportunistic nodes and the radio impact of human beings carrying these devices.

In this paper, we hence strive to answer a simple question: is WiFi-based opportunistic networking feasible with current smartphones. And if yes, what is the performance of WiFi-based opportunistic radio link with those devices in a real-world environment. We start by revisiting the link budget between two smartphones in Section II. Next, we detail the internal characteristics of different smartphones (antenna type and gain, WiFi chipset and output power) in Section III. Then, we report about our line of sight (LoS) outdoor field measurements from which we derive the best path loss model in Section IV. We evaluate the impact of the body attenuation model in Section V, assess the empirical maximum LoS range in Section VI and eventually derive the opportunistic WiFi link capacity of crossing pedestrians. Eventually, we survey related work in Section VII and discuss open points and future work in Section VIII.

The main contributions and findings of this paper are:

- A fully characterized smartphone link budget from their output power to their reception threshold
- A calibrated Two-Ray Ground model and a body model derived empirically
- LoS range measurements with different smartphones, evaluating practical communication range (up to 400m) and goodput of two crossing pedestrians of at least 143 MB

II. Smartphone Link Budget

The link budget generally reflects all gains and losses that RF signals are subjected to while travelling from the transmitter to the receiver. Our methodological teardown will follow the sequence of the individual items of the radio link budget. This gives us a step by step better understanding of the smartphone WiFi properties for opportunistic networking. Opposed to traditional link budgeting, we have no degree of freedom regarding the WiFi parameters on smartphones and have to account for the carrier's body impact on the signal.

978-3-9018-8273-9/15/ ©2015 IFIP

A link budget accounts for all the gains and losses from the transmitter, through the medium to the receiver as illustrated in Figure 1.

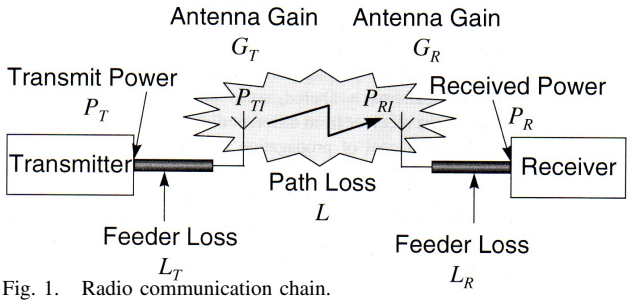

Fig. 1. Radio communication chain.

The link budget equation is given by:

$$P_R = P_T - L_T + G_T - B_T - L - B_R + G_R - L_R \; [dB \; or \; dBm] \quad (1)$$

P_R	received power (dBm)
P_T	transmitter output power(dBm)
L_T	transmitter losses (cable, feeder/connector, ...)(dB)
G_T	transmitter antenna gain (dBd)
B_T	transmitter body attenuation (dB)
L	free space loss or path loss (dB)
B_R	receiver body attenuation (dB)
G_R	receiver antenna gain (dBd)
L_R	receiver losses (cable, feeder/connector, ...) (dB)

The difference between the received signal power, P_R, and the sensitivity of the receiver is referred to as the link margin. The sensitivity of the receiver depends on the signal bandwidth, the type of modulation and the noise level. The WiFi 802.11b/g thermal noise power (or floor) with a channel bandwidth Δf of 20MHz is:

$$P_{dBm} = 10log_{10}(k_B T \Delta f \times 1000) \quad (2)$$

where k_B = is Boltzmann constant ($1.380650410^{-23} J/K$ (Joule/Kelvin)) , Δf is the bandwidth in Hz and T the room temperature t in Kelvins ($T = 273.15 + t$ in Celsius). At $20°C$ the thermal noise power is -100.9 dBm and at -$5°C$ it is - 101.3 dBm and will hence be roughly the same whatever temperature (winter vs. summer) Thermal noise can be approximated by $-174 \; dBm + 10log_{10}(\Delta f)$ resulting in an average noise power of 101 dBm. The signal to noise ratio (SNR) must be of at least 4 dB in order to achieve a bit error rate (BER) of 10^{-2} required for the lowest rate of 802.11b (DSSS - DBPSK). This results in a reception threshold of -97 dBm.

In the remainder of this paper, we will investigate all the above link budget parameters through publicly available data, measurements and provide models whenever possible.

III. Inside Smartphones

Based on publicly available data (e.g. FCC), we report about the position and type of the WiFi antenna and their gains. We then provide a few WiFi chipset characteristic and the radiation patterns of smartphones.

A. Antenna Characteristics

All recent smartphones are equipped with Planar Inverted-F antennas (PiFa) that belong to the family of patch antennas. A PiFa antenna is resonant at a quarter-wavelength thus reducing the required space needed on the phone. With PiFas the entire

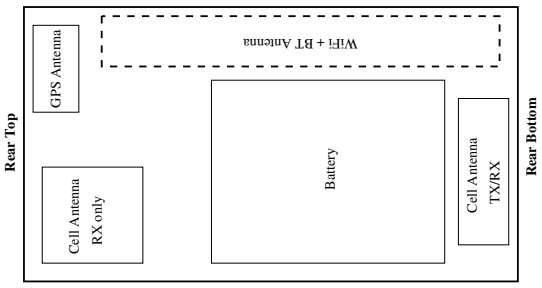

Fig. 2. General layout of the different antennas. The area where the WiFi PiFa are usually located in defined by the dashed rectangle.

Phone Model	WiFi Chipset	Avg. RF Output Power (dBm)
HTC Nexus One	BCM4329	802.11b: 16.85-17.40 dBm
Samsung Galaxy Nexus	BCM4330	802.11b: 15.5-16.5 dBm
Samsung Galaxy SII	BCM4330	802.11b: 17.15 dBm
Samsung Galaxy SIII	BCM4330	802.11b: 16.0-17.12 dBm
Apple iPhone 4S	BCM4330	802.11b: 17.05 dBm

TABLE I. Smartphone WiFi characteristics (source: FCC test reports available at transition.fcc.gov/oet/ea/fccid).

ground plane that supports the circuit board and touch screen (i.e. the entire phone) makes up the antenna. Hence, the bigger the phone, the better. Figure 2 shows the layout of the different antennas as observed on most smartphones (rear view). The GPS antenna is located on top for maximum reception and there are two cell antennas: one at the top but RX only at the top and one at the bottom for TX and RX so that the EM exposure is reduced at the ear level. The WiFi PiFa is always located on the rear's right side and spans almost the whole phone length as shown by the dashed line. Antenna gains reported by the FCC vary from 1.1 dBi for the HTC Nexus One to -2.5 dBi on the the HTC One X and -1.5 dBi on the iPhone 4S.

B. WiFi Chipsets Characteristics and Emitted power

Table I lists the major smartphones with their WiFi chipsets and output power at the chip. We can see that most smartphones use the same chipset and that their average output power is between 16 dBm to 17 dBm for 802.11b. This is 3 dBm below the usual limit of 20 dBm (100 mW). The output power for 802.11g and 802.11n are lower than 802.11b and between 10 dBm and 15 dBm.

The antenna gain will impact the emitted and received power. With PiFa antennas the radiation is away from the ground plane (towards the rear of the phone) and the energy is directed away from the head. This also means that the maximum gain or energy (or best configuration for phones to communicate) is when phones' rear face one another.

Table II shows the surface area and the field intensity E measured by the FCC at the level of the antenna. The Nexus One emits 13 V/m, 5.32 V/m and 10 V/m at the rear, front and side, respectively. We can already see a difference of more than 7 V/m (more than double) between the front and rear. In order to translate the field intensity to the power density P_d, we compute the power density from the field intensity by

$$P_d = \frac{E^2}{Z_0} = \frac{E^2}{120\pi} = \frac{E^2}{377} \; (Watts/m^2) \quad (3)$$

For $E = 13 \; V/m$ (rear), we have $P_d = \frac{13^2}{377} = 0.45 \; W/m^2$ which translate to $-3.5 \; dBW/m^2$. For $E = 5.32 \; V/m$ (front), we have $P_d = -11.2 \; dBW/m^2$ and for the side $E = 10 \; V/m$,

Phone Model	Surface area cm^2	Back V/m	Front V/m (ΔdB)	Side V/m (ΔdB)
Nexus One	71	13.0	5.32 (7.7)	10.8 (1.6)
Galaxy Nexus	92	8.44 (3.75)	4.60 (5.27)	7.3 (1.26)
Galaxy SII	71	8.97 (3.22)	4.82 (5.39)	7.84 (1.17)
Galaxy SIII	96	10.5 (1.85)	3.1 (10.6)	5.17 (6.15)
iPhone 4S	67	11.5 (1.06)	6.61 (4.8)	8.58 (2.54)

TABLE II. PHONE SURFACE AREA AND FIELD INTENSITY (BACK VS. FRONT VS. SIDE). IN BLUE, FOR A GIVEN PHONE, THE LOSS ON OTHER SIDES COMPARED TO THE BACK SIDE. IN RED, DIFFERENCES OF THE DIFFERENT PHONES COMPARED TO THE NEXUS ONE FOR THE BACK.

we have $P_d = -5.76\ dBW/m^2$. This is a difference of almost 8 dB in power density between the rear and the front of the phone and 1.6 dB between the rear and side. From Table II, we see that the power density on the side of the phone is usually very close to the back since the antenna is on the side (except for the iPhone 4S). And differences between 4.8 dB to 10.6 dB can be observed between the rear and the front (screen).

Another observation is that despite all phones having almost the same WiFi chipset and RF output power, they have different effective radiated power from the antenna depending on the side (i.e. rear vs. back. vs. side). This is due to the different antennas used in the different phones, which have different gains and different connector losses.

The still unknown feeder and connector losses between the WiFi chip and the antenna (B_T and B_R) and the propagation loss L will be evaluated using our outdoor measurement results in Section IV.

IV. A REALISTIC SMARTPHONE PROPAGATION MODEL

To obtain realistic values for the smartphone link budget elements, we use extensive outdoor measurements that are presented in this section. The results of the different measurements are then used to derive the feeder and connector losses as well as a realistic path loss model for opportunistic networking in open (e.g. rural) spaces.

A. Experimental Setup

The outdoor measurements took place in Dietikon (AG), Switzerland on a road with 450m of LoS (line of sight) surrounded by fields with low WiFi interferences. A HTC Nexus One acting as an AP was mounted on a tripod at 1.25 m above ground with its rear facing the LoS. An experimenter was holding different smartphones at 1.35 m facing the AP (i.e. rear facing the AP to have maximum antenna gain configuration). The experimenter walked backwards until out of range and then walking forward on the reverse path towards the AP. The experimenter phones acting as RX were receiving WiFi probes sent by the AP acting as a TX and measuring the RSS.

To get precise measurements, we took measurements every 0.5m from [0m,20m] using a meter and then every 10m from [20m,100m] and every 30 to 50m from [100m,350m] using a laser rangefinder ($+/-1m$ accuracy).

B. Propagation Model Fitting

We use the Two-Ray ground model, an extension of the Friis model, which accounts for a direct wave and a ground reflected wave as reference model for our measurements. In the Two-Ray ground model, the total received energy is modeled as the vector sum of the direct transmitted wave and one ground reflected wave. The model used for the propagation of the direct and reflected wave is the Friis model. The two waves are added constructively or destructively depending on their phase difference at the receiver. The magnitude and phase of the direct transmitted wave varies with distance traveled. The magnitude of the reflected wave depends on total traveled distance and the reflection coefficient (Γ) relating the wave before and after reflection. The reflection coefficient mainly depends on the incident angle (Θ_i) and the different dielectrics i.e., permittivity (ε_r or E_r), permeability (μ_r) and conductivity (σ). We consider $\mu_r = \sigma = 1$ and $\varepsilon_r = 12$ for the ground reflection coefficient.

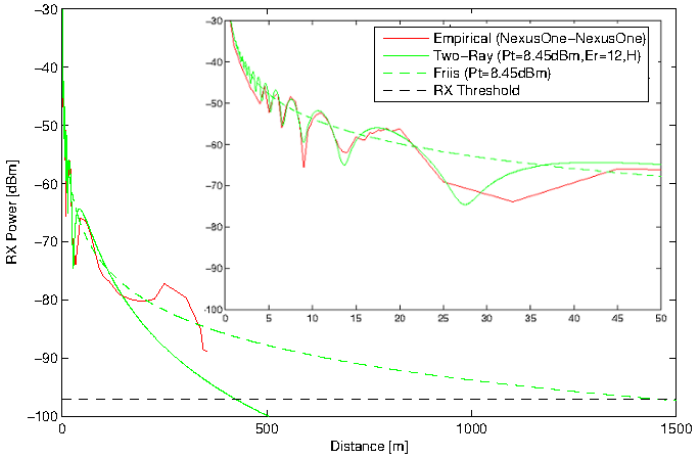

Fig. 3. Measurements with two HTC Nexus Ones fitted with the Two-Ray and Friis model.

The Figures 3 show the empirical measurements and the best fit with the Two-Ray model. They also show the Friis model with the parameters corresponding to the Two-Ray fit. At the long range behavior where $d \gg h_{TX} + h_{RX}$ in Figure 3 we can clearly see the impact of the reflected wave which drastically limits the reception range. The horizontal line at -97 dBm indicates the RX sensitivity threshold. This means that in ideal LoS free space conditions, one could detect beacons up to 1200 or 1500 m.[1] Due to the reflected wave on the ground (in phase opposition) for a horizontal LoS, this range reduces to 380-450m. The zoomed part shows the fit for the short range behavior 0-50m where $d > h_{TX} + h_{RX}$. The Two-Ray model was fitted with the following parameters: $Er = 12$, $h_{Rx} = 1.25m$, $h_{TX} = 1.35m$, $G_{TX} = G_{RX} = 1.1dBi$. The green plain line is the best fit with $P_{TX} = 7mW$ (8.45 dBm). The dashed green line is the corresponding Friis model with the same parameter. We can clearly see the impact of the ground and the difference between the RX signal power predicted by the Friis model and the Two-Ray mode. At short ranges the two-ray fit is striking. The signal experiences deep fades of up to 10 to 15 dB.

The Two-Ray model does not however fit the empirical data for the long-range part from 175m to 350m where one can oberve a bump. This is due to the road going slightly up from 200 to 300m, which increases the reflection angle and the height of the carried phone. With the Two-Ray model, increasing the height of either TX or RX drastically increases the range and allows coming closer to free space propagation (Friis model). Similar to the deep fades observed

[1]This was confirmed by a joint Uepaa/Rega experiment with a phone on the ground and another hooked below a helicopter going up vertically.

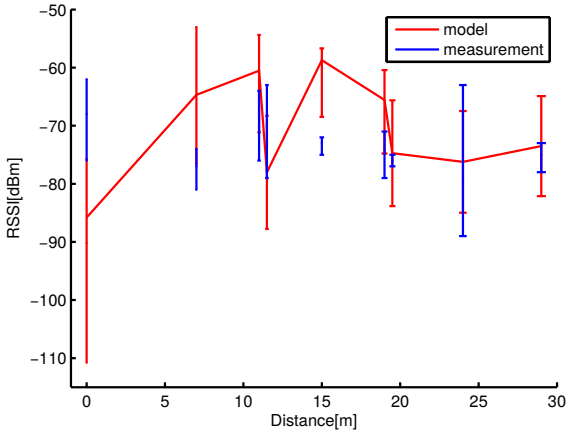

Fig. 4. Body attenuation measurements.

at short ranges due to destructive signals, this bump is due to constructive signals.

C. Feeder and Connector Losses

Fitting the two-ray ground model to our measurements outputs a P_T of 7 dBm as opposed to 17 dBm reported by the FCC (see Table I). The difference of 10 dBm is due to the feeder and connector losses from the WiFi chip to the PiFa antenna. Based on our output power estimation by the model fitting, we conclude that the combined feeder and connector losses for sender and receiver are on the order of 10dB (L_T+L_R). Thus the combined feeder and connector losses for the transmitter or receiver are 4-5 dB. The maximum range measurements reported in section VI confirm those losses. For these range tests, we used a Samsung Galaxy Nexus as an AP and different phones as stations. The different phones could detect the AP beacons until different distances from the transmitter. Since TX was the same accross all tests (i.e. same P_t and G_t) and the WiFi chipset of all RX phones are the same (i.e. BCM4330 - see Table I), the observed range difference can only be explained by different antenna gain G_R and connector/feeder losses L_R.

V. Body Attenuation

In this section, we investigate the impact of the smartphone carrier's body on the link budget.

A. Body attenuation Model and Measurements

During our early field measurements, we noticed the impact of the body attenuation on the received signal strength. The attenuation of the body blocking the LoS is often neglected when considering signal propagation involving mobile devices. When computing the attenuation of human tissue, we see that the attenuation is significant. First, part of the wave hitting the body is reflected and part absorbed. According to the body reflection coefficient, 80% to 90% of the wave is reflected for an incident angle of 90 degrees. The remaining 10% to 20% of the absorbed energy experiences loss due to velocity change at the air/body interface

$$L_\alpha = 20\log_{10}\left(\frac{\lambda_0}{\lambda}\right) = 20log10\left(\frac{\frac{c}{f}}{\frac{2\pi}{\beta}}\right) = 20log10\left(\frac{c}{f}\frac{\beta}{2\pi}\right) \quad (4)$$

Then, the propagation losses through through the body are

$$L_\beta = 20\log_{10}\left(e^{\alpha d_{body}}\right) = 20\frac{\ln(e^{\alpha d_{body}})}{\ln(10)} = \frac{20}{\ln(10)}\alpha d_{body} \quad (5)$$

where d_{body} is the distance the signal travels though the body.

	Relative Permittivity	Conductivity	α	β
Torso	39.2	1.8	53.5	320.7
Head	52.7	1.95	50.2	369.5

TABLE III. Dielectric properties of human tissue [10].

Both equations use the dielectric constants reported in Table III according to the tissue equivalent material defined in [10] for RF dosimetry measurements at 2.4GHz. α and β are the real and complex components of the propagation constant γ ($\gamma = \alpha + j\beta$). A numerical evaluation of the resulting attenuation due to the propagation through the body gives 5 dB/cm of attenuation. Communication from the front to the back of the body through the body is therefore impossible since the signal would be attenuated below the reception threshold.

Another additional propagation effect comes into play: diffraction around the body. The rays traveling around the body due to diffraction suffer a noticeably smaller attenuation. The attenuation of waves which are diffracted around the body has mainly been studied in the context of body area networks, where antennas are placed on or near the body. [11] reports an attenuation in the order of 2 dB/cm at 2.4 GHz.

We hence consider these values to estimate the attenuation due to diffraction around the modeled body. The body is assumed to be a perfect cylinder with a radius of 15 cm and with the dielectric properties of Table III. The attenuation of the body with a source away from the body and a receiver on or close to the body is then computed according to two rays being diffracted around the body, one around the top and one around the bottom of the body as shown in the Figure with the two dashed lines.

We carry measurements to validate this model. We used two helium balloons to position the transmitting phone in the air and measure the attenuation of the body with a receiving phone placed on the experimenter's body. The balloons were moved away from the body at a height of 15m to 20m. For each measurement point the distance from the person lying on the ground and the height of the balloon was measured. As can be observed in Figure 4, the variation of the measurements is very large. Due to the wind, the position of the balloon could not be controlled perfectly. Therefore the measured distances do not exactly correspond to the actual distances during the measurements. We hence accounted in the model for a variation in transmitter position of 1m in each direction. Since the body is not an actual cylinder, the placement on the model cylinder had to be estimated, therefore a variation on the position of the phone on the model cylinder of 15° was also taken into account for the model. This shows that the body attenuation model is also strongly variable with small changes of position. We can see that the model generally overestimates the measurements. This is due to the neglected orientation and polarization mismatch because of the relative position of the phones. Therefore we use an additional 10dB of attenuation in the model to account for the orientation losses due to the phone being carried on the body in order to eventually match the measurements. The bottom line is that we consider our

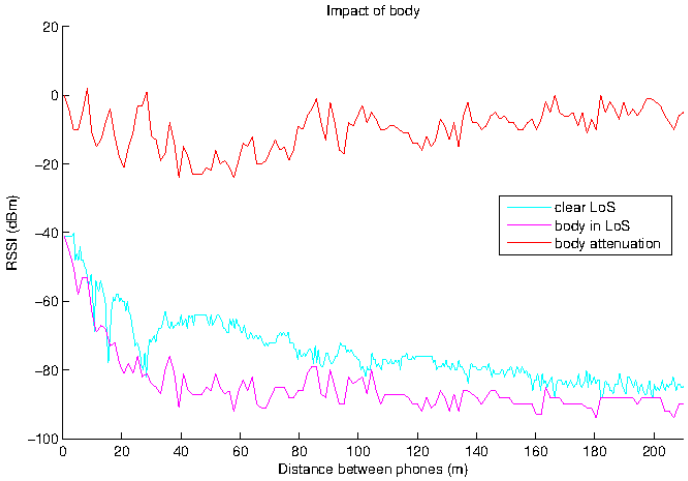

Fig. 5. LoS measurements w/ and w/o body.

Phone	Out of range (backwards)	Within range (forward)
Galaxy Nexus	420m	358m
Galaxy S II	300m	270m
Galaxy S III	435m	405m

TABLE IV. BEACON RECEPTION RANGE.

measurements to confirm the 2 dB/cm diffraction losses at 2.4 GHz.

B. LoS measurements with and without body attenuation

Measurements for the body attenuation were taken while slowly and continuously walking away from the access point phone. GPS was used as additional sensor to allow for more fine-grained empirical plots. Figure 5 shows the received signal strength with and without the body attenuation as well as the difference between the two at the top. A first observation is that the body attenuates the signal by a maximum of 20 dB and that the resulting measurements follow almost the same trend as the measurements without the body. Regarding long ranges, we can see observe that the difference between the two measurements tends to zero with distance. This is due to the fact that the further away from the AP, the less distance both waves (direct and reflected) have to travel around the body. At 100m we observe almost a 20 dB difference, which suggests a distance of 10cm traveled by the diffracted wave around the body. At 150m, we only have 10 dB difference suggesting that the distance traveled around the body is half i.e., 5cm.

VI. MAXIMUM RANGE AND LINK CAPACITY

Now that we have characterized all smartphone link budget elements, we will try to answer the following question: "How much goodput can be achieved in a typicall opportunistic networking scenario". To be precise, we will estimate the goodput of the contact when two pedestrians are walking past each other in opposite directions. We carried out further measurements to assess the maximum communication range and rates for different smartphones.

A. Maximum Range

We first walked backwards (facing the AP) until we lost connectivity to the AP and then walked back (forward) towards the AP. Table IV gives the range at which the different phones were still able to receive WiFi beacons.

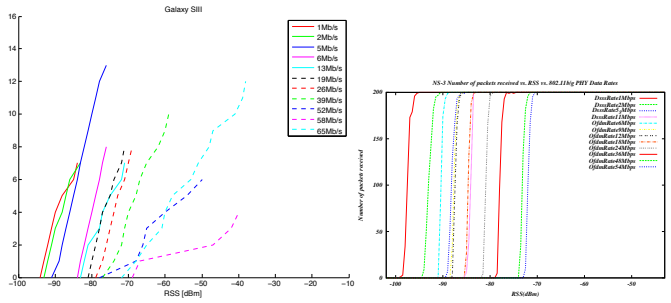

(a) Galaxy SIII (b) NS-3

Fig. 6. 802.11 PHY data rates vs. RSSI for Galaxy S III and NS-3.

We can observe two things: **Range Heterogeneity over different phone models**: This is clearly due to the difference in antenna characteristics since most devices embed the same WiFi chipset with similar performances (see Table I). An additional important factor is the size of the phone and the antenna placement. This is highlighted by the Galaxy SIII which exhibits the largest range despite average values for its EM field on the different phone sides. Its size allows to have a larger ground plane (i.e. entire phone comprising the board and touchscreen) for the PiFa antenna coming close to the half-wavelength (6.1 cm) or wavelength (12.2 cm) of WiFi 2.4 GHz required to radiate EM with maximal gain. Also due to its size, less surface was covered with the experimenters hand and hence more power was received.

Asymmetry of In- and Out-range Border for the same phone: This range difference can be explained by the fact that when out of range, the device has to discover the AP by active probing (scanning with Probe Requests). The default period at which devices look for available APs might be too large for our scenario. By reproducing the experiment and looking at the behavior of a Nexus One, a SII and a SIII, we found that phones only scan from time to time when they lost connection to the current AP.

B. 802.11 PHY Data Rates

In addition to the maximum range, we need information about the rates (MCS) at which data was sent depending on the distance and SNR. Using the same measurement procedure as described above, we plot the 802.11 PHY rates vs. RSSI for a Samsung Galaxy S III phone as shown in Figure 6. We used a Galaxy S III as it implements 802.11n and is currently one of the most widely spread Android smartphones. We also plot the 802.11 PHY rates as implemented in NS-3 vs. RSSI (and additionally the number of packets successfully decoded (i.e. with no bit errors) per RSSI and data rate). Note that the NS-3 simulator was calibrated with chip/bit error rate formulas relative to the different modulation as reported in [12].

The overall behavior is as expected i.e. data rates correlate with the RSSI and the better the RSSI, the higher the data rate. The empirical data rates show similar behaviors across the different phones. The theoretical models of the data rates as implemented in NS-3 are ordered according to the RSSI. The empirical behavior as shown by the WiFi chipsets show less consistent and predictable behaviors as the MCS sequence order is not always respected.

C. Opportunistic WiFi Link Capacity of Crossing Pedestrians

Based on our evaluation, we are finally interested in the data transfer capacity while two pedestrians are crossing. In

order to reflect the currently typical WiFi 802.11n standard implemented on smartphones, we base our capacity estimation on the data rates that we measured with a Samsung Galaxy S III phone. Measurements were taken using UDP unicasts sent from the moving phone to the fixed access point phone. The data rates of received packets were recorded at the access point phone. This was done for approaching the access point (without body in between) and for walking away from the access point (with two user bodies in LoS) and thus one data rate series was obtained for each part of the crossing. To model the impact of different walking speeds, we calculate the relative fraction of time spent at each data rate for each part of the pedestrians crossing. The incoming transmission range is based on our measurements set to 350m and the range after the crossing is set to 80m. With the communication ranges obtained by our measurements we can estimate the capacity for different walking speeds. We assume that a variation of walking speed of +/- 0.2 m/s does not impact the 802.11 rate adaption. For walking speeds of 0.8 m/s (2.88 km/h or 1.79 mph), 1 m/s (3.6km/h or 2.24 mph) and 1.2 m/s (4.32 or 2.68mph) we get an estimated goodput of 214, 171 and 143 MB respectively, taking the WiFi overhead and the packet errors we measured into account.

VII. Related Work

In this section we complement the information about related work that is already given directly in the previous sections. In [13] the authors address the directionality of smartphone antennas by proposing a multi antenna system that selects the best available antenna for the current transmission. Directional antennas in simulations was investigated in [14]. There are many commonly used propagation models that can also be applied to WiFi signals e.g. [15]. A survey of propagation models is given in [16]. [17] specifically use a propagation model based on frensel zones that takes the frequency and antenna height of smartphones into account. However, it neglects the fluctuations that we observed in our measurements which can be modeled by the two-ray ground model. Smartphone-based WiFi behavior is of interest, as in [18] a distance througput model, that takes connection set up times into account is presented, however the body attenuation is not considered. The authors also show, that the DHCP discover process takes a significant time, which confirms the observation in our own measurements, that the communication range while walking towards an AP is lower than while walking away.

VIII. Discussion and Conclusion

In this paper, we investigated the feasibility of opportunistic communications using modern smartphones. We conducted a methodological study to evaluate smartphones' WiFi performance. First, we systematically characterized the smartphone link budget elements (antenna, WiFi chipset). We then focused on the case of two smartphones in outdoor LoS carried by pedestrians crossing in a low WiFi interference environment. We have found that body attenuation, usually overlooked in classical link budget formulation, can have an important impact since smartphones since are carried close to the body or hold in the hand. Furthermore, we have demonstrated empirically and validated through the Two-Ray propagation model that smartphones can communicate from 300m to 450m. This results in a goodput of 143 MB for crossing of two pedestrians walking at 4.3 km/h. Eventually, an important finding is that the WiFi range is limited by the destructive ground reflective wave and that ideal LoS propagation could achieve more than 1km with current smartphones.

Due to space restriction, we did not report about the impact of the relative phones orientation and the related antenna's horizontal vs. vertical polarization. We did not also investigate further the possibility for asymmetric links to happen due to the heterogeneous characteristic and performance of different smartphones. Nonetheless, we believe our study already proves the feasibility of opportunistic networking in rural area based on current smartphones' capabilities.

Most opportunistic contacts in rural areas will happen in social places such as villages or markets with a mid- to high-density of smartphones. There, interference will play a higher role on impacting the capacity of opportunistic networking. For future work we hence plan to evaluate high-density scenarios through real-world experiments and simulations. We are currently integrating all the findings of this paper to improve the NS-3 simulator.

References

[1] A. Chaintreau *et al.*, "Pocket switched networks: real-world mobility and its consequences for opportunistic forwarding," University of Cambridge, Tech. Rep., 2005.

[2] G. Karlsson, V. Lenders, and M. May, "Delay-Tolerant Broadcasting," *Broadcasting, IEEE Transactions on*, vol. 53, no. 1, pp. 369–381, 2007.

[3] B. Han *et al.*, "Cellular traffic offloading through opportunistic communications: a case study," in *CHANTS*, 2010.

[4] T. Hossmann *et al.*, "Twitter in disaster mode: security architecture," in *SWID*, 2011.

[5] S. Guo *et al.*, "Very low-cost internet access using KioskNet," *ACM SIGCOMM Computer Communication Review*, 2007.

[6] "Eu fp7 n4c project - networking for communications challenged communities," http://www.n4c.eu/.

[7] "Twimight: Twitter client with disaster mode," www.twimight.com.

[8] "Uepaa! - alpine safety app," http://www.uepaa.ch/.

[9] "Opengarden's firechat app," https://opengarden.com/firechat.

[10] M. Y. Kanda *et al.*, "Formulation and Characterization of Tissue Equivalent Liquids Used for RF Densitometry and Dosimetry Measurements," *IEEE Transactions on microwave theory and techniques*, 2004.

[11] A. Fort *et al.*, "A Body Area Propagation Model Derived From Fundamental Principles: Analytical Analysis and Comparison with Measurements," *IEEE Tran. on Antennas and Propagation*, 2010.

[12] G. Peu and T. Henderson, "Validation of NS-3 802.11b PHY model." New York, USA: Boeing Research and Technology, 2009.

[13] A. Amiri Sani, L. Zhong, and A. Sabharwal, "Directional antenna diversity for mobile devices," in *MobiCom '10*, New York, USA, 2010.

[14] E. Anderson *et al.*, "The impact of directional antenna models on simulation accuracy," in *Wi-Opt '09*. IEEE, 2009.

[15] M. Hata and B. Davidson, "A report on technology independent methodology for the modeling, simulation and empirical verification of wireless communications system performance in noise and interference limited systems operating on frequencies between 30 and 1500 mhz," in *Working group*, 1997.

[16] C. Phillips, D. Sicker, and D. Grunwald, "A Survey of Wireless Path Loss Prediction and Coverage Mapping Methods," *IEEE Communications Surveys & Tutorials*, vol. 15, no. 1, pp. 255–270, 2013.

[17] D. Green and A. Obaidat, "An accurate line of sight propagation performance model for ad-hoc 802.11 wireless LAN (WLAN) devices," in *ICC '02*, vol. 5. IEEE, 2002.

[18] S. Seneviratne *et al.*, "Characterizing WiFi connection and its impact on mobile users," in *WiNTECH '13*, New York, USA, 2013.